



Published in final edited form as:

Neurobiol Dis. 2021 March ; 150: 105237. doi:10.1016/j.nbd.2020.105237.

Mural cell dysfunction leads to altered cerebrovascular tau uptake following repetitive head trauma

Joseph Ojo^{a,b}, Max Eisenbaum^{a,b}, Ben Shackleton^{a,b}, Cillian Lynch^{a,b}, Utsav Joshi^{a,b}, Nicole Saltiel^a, Andrew Pearson^{a,b}, Charis Ringland^{a,b}, Daniel Paris^{a,b}, Benoit Mouzon^{a,b}, Michael Mullan^{a,b}, Fiona Crawford^{a,b,c}, Corbin Bachmeier^{a,b,d,*}

^aThe Roskamp Institute, Sarasota, FL, USA

^bThe Open University, Milton Keynes, UK

^cJames A. Haley Veterans' Hospital, Tampa, FL, USA

^dBay Pines VA Healthcare System, Bay Pines, FL, USA

Abstract

A pathological characteristic of repetitive traumatic brain injury (TBI) is the deposition of hyperphosphorylated and aggregated tau species in the brain and increased levels of extracellular monomeric tau are believed to play a role in the pathogenesis of neurodegenerative tauopathies. The pathways by which extracellular tau is eliminated from the brain, however, remains elusive. The purpose of this study was to examine tau uptake by cerebrovascular cells and the effect of TBI on these processes. We found monomeric tau interacts with brain vascular mural cells (pericytes and smooth muscle cells) to a greater extent than other cerebrovascular cells, indicating mural cells may contribute to the elimination of extracellular tau, as previously described for other solutes such as beta-amyloid. Consistent with other neurodegenerative disorders, we observed a progressive decline in cerebrovascular mural cell markers up to 12 months post-injury in a mouse model of repetitive mild TBI (r-mTBI) and human TBI brain specimens, when compared to control. These changes appear to reflect mural cell degeneration and not cellular loss as no difference in the mural cell population was observed between r-mTBI and r-sham animals as determined through flow cytometry. Moreover, freshly isolated r-mTBI cerebrovessels showed reduced tau uptake at 6 and 12 months post-injury compared to r-sham animals, which may be the result of diminished cerebrovascular endocytosis, as caveolin-1 levels were significantly decreased in mouse r-mTBI and human TBI cerebrovessels compared to their respective controls. Further emphasizing the interaction between mural cells and tau, similar reductions in mural cell markers, tau uptake, and caveolin-1 were observed in cerebrovessels from transgenic mural cell-depleted animals. In conclusion, our studies indicate repeated injuries to the brain causes chronic mural cell degeneration, reducing the caveolar-mediated uptake of tau by these cells. Alterations in tau uptake by vascular mural cells may contribute to tau deposition in the brain following head trauma and could represent a novel therapeutic target for TBI or other neurodegenerative disorders.

This is an open access article under the CC BY-NC-ND license (<http://creativecommons.org/licenses/by-nc-nd/4.0/>).

*Corresponding author at: 2040 Whitfield Avenue, Sarasota, FL 34243, USA., cbachmeier@roskampinstitute.org (C. Bachmeier).

Declaration of Competing Interest

None.

Keywords

Mural cells; Tau; Pericytes; Smooth muscle cells; Traumatic brain injury; Alzheimer's disease; Caveolin-1

1. Introduction

Traumatic brain injury (TBI) is the result of a sudden trauma to the brain that significantly disrupts brain function (Blyth and Bazarian, 2010). One of the long-term consequences of repetitive head trauma is the accumulation of hyperphosphorylated tau (Stern et al., 2011) and the presence of tau-reactive neurofibrillary tangles (Blaylock and Maroon, 2011) and neuropil threads (Omalu et al., 2011). Elevated levels of phosphorylated tau have also been observed in various animal models of TBI by our group (Ojo et al., 2013; Ojo et al., 2016) and others (Goldstein et al., 2012; Huber et al., 2013; Petraglia et al., 2014; Zhang et al., 2014). Tau is a cytoplasmic protein which is believed to be restricted to the intracellular compartment of neurons, except when released from dead or degenerating cells. However, more recent work has shown that tau is constitutively released into the extracellular environment under normal conditions (Chai et al., 2012; Karch et al., 2012), indicating tau secretion may be a common biological function (Medina and Avila, 2014). Furthermore, several studies have indicated tau pathology is propagated through extracellular tau spreading and it is believed that increased levels of monomeric tau in the extracellular environment play a major role in the pathogenesis of neurodegenerative tauopathies (Le et al., 2012; Michel et al., 2013). In fact, tau elevations in the brain extracellular space can be used to predict adverse clinical outcomes following TBI (Magnoni et al., 2012; Ost et al., 2006).

Despite the prevalence and importance of extracellular tau in normal and disease conditions, there is little understanding of how extracellular tau is processed and eliminated from the brain. A study recently demonstrated that extracellular tau is eliminated from the brain through paravascular pathways (Ilf et al., 2014). A common paravascular pathway for removing solutes from the brain involves uptake and degradation by brain vascular mural cells (pericytes and smooth muscle cells). Prior studies have shown mural cells contribute to the elimination of beta-amyloid (A β) from the brain, (Alcendor, 2020; Kanekiyo et al., 2012; Kirabali et al., 2019; Ma et al., 2018), which accumulates in the brains of Alzheimer's disease (AD) patients (and to a lesser extent in TBI subjects) (Tsitsopoulos and Marklund, 2013). Studying the role of brain vascular mural cells in tau uptake may be particularly relevant in head trauma as a prominent feature of TBI is the presence of perivascular tau tangles (Stern et al., 2011; McKee et al., 2009). Moreover, recent work found that paravascular tau clearance was reduced by approximately 60% following TBI and was associated with phospho-tau pathology and neurodegeneration (Ilf et al., 2014).

Mural cell loss in the brain vasculature is a common feature of many neurodegenerative disorders including AD (Bourassa et al., 2020; Sagare et al., 2013; Sengillo et al., 2013) and Amyotrophic Lateral Sclerosis (ALS) (Winkler et al., 2013), with more modest reductions also occurring in the course of normal aging (Bell et al., 2010). With respect to TBI, pericyte

loss has been observed acutely following a single controlled cortical impact (Choi et al., 2016; Zehendner et al., 2015) and, more recently, several pericyte markers were found to be significantly reduced after fluid percussion injury in mice (Bhowmick et al., 2019), though more chronic time points have yet to be examined. The degeneration of mural cells in the brain may explain the progressive solute accumulation that is prevalent in neurodegenerative disorders (e.g., A β in AD, transactive response DNA binding protein 43 (TDP43) in ALS, and pathologic tau in repetitive TBI). Furthermore, as changes in brain caveolin-1 levels have recently been shown to correlate with tau disposition in the brain (Bonds et al., 2019; Head et al., 2010), we examined caveolin-1 expression alongside tau uptake in isolated cerebrovessels. At this stage, the role of mural cells in tau uptake is poorly understood, and the long-term effects of repetitive head trauma on mural cells in the brain has yet to be fully investigated. Since these cells can be important mediators of solute disposition and accumulation in the brain, the purpose of the present study was to evaluate the interaction between tau and brain vascular mural cells and determine the status of these cells chronically following repetitive brain injury.

2. Materials and methods

2.1. Materials

Brain vascular pericytes (cat#1200), brain vascular smooth muscle cells (SMC) (cat#1100), brain microvascular endothelial cells (HBMEC) (cat#1000), astrocytes (cat#1800), and microglia (cat#1900) (all of human origin) and associated culture reagents were purchased from Sciencell Research Laboratories (Carlsbad, CA, USA). Fibronectin solution (cat#F1141), poly-L-lysine solution (cat#P4707), collagenase/dispase (cat#11097113001), and Hanks' balanced salt solution (HBSS) (cat#H8264) were purchased from MilliporeSigma (St. Louis, MO, USA). Recombinant human tau-441 (rhtau) (cat#T-1001) and fluorescein-labeled A β (1–42) (cat#A-1119) was purchased from rPeptide (Watkinsville, GA, USA). Lucifer yellow dextran (10 kD) (cat#D1825) and the human tau enzyme linked immunosorbent assay (ELISA) (cat#KHB0041) were purchased from Invitrogen Corp. (Carlsbad, CA, USA). The ELISA kits for human (cat#LS-F13051) and mouse (cat#LS-F21849) alpha smooth muscle cell actin (α SMC-actin) were purchased from LifeSpan BioSciences, Inc. (Seattle, WA, USA). The ELISA kits for human (cat#EHPDGFRB) and mouse (cat#MBS919047) PDGFR β (platelet-derived growth factor receptor beta) were purchased from ThermoFisher Scientific (Waltham, MA, USA) and MyBioSource, Inc. (San Diego, CA, USA), respectively. Antibodies for N-aminopeptidase, CD13 (cat#558744), and the brain endothelial cell marker, CD31 (cat#561410), were purchased from BD Biosciences (San Jose, CA, USA). Mammalian protein extraction reagent (M-PER) (cat#78505), Halt enzyme inhibitor cocktails (cat#78442), and the bicinchoninic acid (BCA) protein assay (cat#23225) were purchased from ThermoFisher Scientific (Waltham, MA, USA).

2.2. Animals

Human tau (hTau) mice (cat#005491) were purchased from the Jackson Laboratory (Bar Harbor, ME, USA). The hTau mice express six isoforms of human tau on a C57BL/6 background, but do not express murine tau, as previously described (Andorfer et al., 2003). Transgenic PS1/APPsw (PSAPP) mice overexpressing the “Swedish” mutation (APP695)

and mutant presenilin-1 (M146L) were used as a mouse model of Alzheimer's disease (Holcomb et al., 1998). The mural cell-depleted animals, PDGFR β (+/-), were kindly provided by Dr. Richard Daneman (University of California, San Diego, La Jolla, CA) and were generated by disrupting PDGFR β signaling, which leads to progressive reductions in the vascular expression of smooth muscle cells and pericytes (Bell et al., 2010; Tallquist et al., 2003). All studies used male and female mice, housed under standard laboratory conditions (23 ± 1 °C, $50 \pm 5\%$ humidity, and a 12-h light/dark cycle) with free access to food and water throughout the study. All experiments using animals were performed under protocols approved by the Institutional Animal Care and Use Committee (IACUC) of the Roskamp Institute.

2.3. Brain injury protocol

To investigate the effects of repetitive mild traumatic brain injury (r-mTBI), we used a mouse model of closed head injury as previously characterized by our group (Mouzon et al., 2012; Mouzon et al., 2014). Briefly, animals were secured in a mouse stereotaxic apparatus (Stoelting) mounted with an electromagnetic controlled impact device (Leica) and anesthetized with 1.5 l/min of oxygen and 3% isoflurane. Prior to impact, a 5 mm blunt metal impactor tip was retracted and positioned midway in relation to the sagittal suture. The injury was triggered using the myNeuroLab controller (Leica) at a strike velocity of 5 m/s, strike depth of 1.0 mm, and a dwell time of 200 milliseconds. Mice (3 months of age) received 2 injuries per week for 3 months. In this closed head injury model, there are no incisions and no craniotomy. The mouse head is shaved and the skin is retracted on either side of the brain. The impact is delivered directly to the skin on the midline of the skull. As a control, sham animals did not receive the brain injury, but were exposed to anesthesia for the same length of time as the injured mice and under the same paradigm (2 exposures per week for 3 months). Mice were euthanatized at 24 h, 3 months, 6 months, and 12 months after the final brain injury or anesthesia exposure. A timeline of the injury paradigm and the timepoints for tissue collection are depicted in (Fig. 1).

2.4. Peptide preparation

Using a standard process to limit aggregation, as we previously described (Bachmeier et al., 2013), lyophilized A β peptides were solubilized in 1,1,1,3,3,3-hexafluoro-2-propanol (HFIP) to acquire a monomeric/dimeric sample and minimize the formation of β -sheet structures. Briefly, 1 mg of each lyophilized peptide was dissolved in 1 ml of ice cold HFIP. The peptides were allowed to air dry in a chemical fume hood for one hour followed by further drying in a speed-vac centrifuge for 30 min. The resulting clear film was re-suspended in 100% dimethylsulfoxide to a concentration of 1 mM and stored in aliquots at -80 °C. Recombinant human tau-441 (50 μ g) was dissolved in 1 ml of HBSS and stored in aliquots at -80 °C.

2.5. Tau uptake in vitro

All cells (pericytes, SMC, HBMEC, astrocytes, and microglia) were individually seeded at 50,000 cells per cm^2 onto fibronectin-coated or poly-L-lysine-coated 24-well plates. Upon confluency, cells were treated with rhtau (0.5, 5, and 50 ng/ml) for 1 h at 37 °C. Following the treatment period, the extracellular media was removed, and the cell monolayer washed

with ice-cold HBSS. Cell lysates were collected using lysis buffer (M-PER) supplemented with phenylmethanesulfonyl fluoride (1 mM) and Halt protease and phosphatase inhibitor cocktail. The cell lysates were analyzed for total tau content by ELISA and normalized to total protein content using the BCA protein assay. It should be noted that significant tau degradation is not expected to occur within the time frame of the tau uptake studies. That said, a limitation of this approach is that any tau fragments that may be produced would not be distinguished and any disruptions to the tau epitope could prevent tau detection by the ELISA antibody altogether.

2.6. Isolation of brain fractions

Various brain fractions, including the cerebrovasculature, were isolated from mouse brain tissue as characterized and described by our group previously (Bachmeier et al., 2014). Briefly, the entire mouse brain (minus the cerebellum and brain stem) was freshly collected (300 mg) and ground in ice-cold HBSS with 6–8 passes of a Teflon pestle in a glass Dounce homogenizer. An equal volume of 40% dextran solution was added to the brain homogenate for a final concentration of 20% dextran and immediately centrifuged at 6000g for 15 min at 4 °C. This procedure results in a pellet at the bottom of the container (cerebrovasculature) and a compact mass at the top of the solution (parenchyma) separated by a clear dextran interface (soluble fraction, i.e., noncell associated). As we are interested in the response of both pericytes and smooth muscle cells, we used whole vascular preparations, containing vessels of a variety of sizes (microvessels, arterioles, etc.). As a result, in addition to mural cells, these preparations likely contain brain endothelia and potentially astrocytes. The freshly isolated cerebrovessels were collected and immediately used for the *ex vivo* studies described below.

2.7. Tau uptake, mural cell marker and caveolin-1 expression *ex vivo*

In line with the *in vitro* studies above, tau uptake was evaluated in cerebrovessels isolated from 1) r-mTBI (24 h, 3 months, 6 months, and 12 months post-last injury), 2) PDGFR β (+/-) (12 months of age), and 3) PSAPP (18 months of age) mice. The PDGFR β (+/-) and PSAPP animals were examined at 12 months and 18 months of age, respectively, as prior reporting has shown mural cell disruption at these ages or younger (Sagare et al., 2013; Bell et al., 2010). Additionally, these ages match the respective ages of the r-mTBI animals at 6 and 12 months post-last injury, which allows for comparisons of mural-cell dysfunction between the mouse models while excluding age as a confounding factor. The sample sizes for the r-sham and r-mTBI groups were the same for each timepoint: 24 h ($n = 5$), 3 months ($n = 4$), 6 months ($n = 6$), and 12 months ($n = 4$). The sample sizes for the PDGFR β (+/-) and wild-type littermate groups were $n = 4$ each, while the PSAPP and wild-type littermate groups were $n = 6$ each. Freshly isolated cerebrovessels were treated with 5 ng/ml rtau for 1 h at 37 °C, which is the reported concentration of tau in human ISF (Magnoni et al., 2012; Marklund et al., 2009). In addition, cerebrovessels isolated from a separate cohort of r-mTBI animals at 12 months post-injury were treated with either 2 μ M fluorescein-labeled A β (1–42) or 10 μ M lucifer yellow dextran for 1 h at 37 °C. For this study, the sample sizes for the r-sham and r-mTBI groups were the same for each probe: lucifer yellow dextran ($n = 4$), fluorescein-labeled A β 1–42 ($n = 5$). Following the treatment period, the extracellular media was removed, and the cerebrovessels were washed with ice-cold HBSS. Cell lysates were

collected using lysis buffer (M-PER) supplemented with phenylmethanesulfonyl fluoride (1 mM) and Halt protease and phosphatase inhibitor cocktail. The cell lysates were analyzed for total tau content, α SMC-actin, PDGFR β , and caveolin-1 by ELISA, while the fluorescein-labeled A β (1–42) and lucifer yellow dextran were analyzed using a microplate fluorescence reader. All samples were normalized to total protein content using the BCA protein assay.

2.8. Mural cell marker and caveolin-1 expression in human brain specimens

Human brain specimens were acquired from Dr. Thomas Beach, Director of the Brain and Body Donation Program at the Sun Health Research Institute (Sun City, AZ). Frozen human cortex samples from the inferior frontal gyrus (500 mg) were obtained from the autopsied brains of 1) non-demented control subjects (no history of TBI or AD diagnosis), 2) TBI, 3) AD, and 4) TBI and AD. For the TBI specimens, donors reported 1 or 2 brain injuries in which loss of consciousness occurred and each incident lasted less than 30 min. Moreover, as we are primarily interested in the chronic phase post-injury, samples with a longer post-last injury period were prioritized (mean, ~40 years post-last injury). A summary of the human brain specimens is displayed in Table 1. In the same manner as the mouse *ex vivo* studies above, the cerebrovasculature was isolated from each human brain specimen and collected using lysis buffer (M-PER) supplemented with phenylmethanesulfonyl fluoride (1 mM) and Halt protease and phosphatase inhibitor cocktail. The cell lysates were analyzed for α SMC-actin, PDGFR β , and caveolin-1 by ELISA and normalized to total protein content using the BCA protein assay.

2.9. Flow cytometry

Fresh cerebrovascular tissue was isolated from the brains of r-sham and r-mTBI mice at 6 months post-last injury and processed as previously described (Crouch and Doetsch, 2018). Briefly, the cerebrovascular pellet (obtained as described above) was resuspended in a collagenase/dispase solution (1 mg/ml) and incubated for 1 h at 37 °C with gentle agitation. Following enzymatic digestion, the tissue was pelleted by centrifugation at 6000 rpm for 3 min and resuspended in a DNase solution (1 mg/ml, Worthington Biochemical) and subjected to further mechanical digestion via trituration with a pipette to achieve a single cell suspension. The tissue was centrifuged at 6000 rpm for 3 min, the supernatant discarded, and the resulting pellet was resuspended and stained with antibodies against the mural cell-specific N-aminopeptidase (CD13) using anti-CD13-FITC at 1:200 (BD Biosciences), and the brain endothelial cell marker (CD31) using anti-CD31-PE-CY7 at 1:500 (BD Biosciences). For live/dead cell discrimination, the viability dye propidium iodide (Sigma Aldrich) was added to the antibody cocktail. Cells were stained on ice for 30 min in the dark and resuspended in 1% BSA in HBSS. Data were acquired and analyzed using the Attune® NxT Acoustic Focusing Flow Cytometer and Attune® NxT software version 2.7 (Thermo Fisher Scientific, Waltham, MA, USA).

2.10. Statistical analyses

Quantitative data were plotted as mean \pm standard error of the mean. Statistical analysis was performed using InStat 3.0 or GraphPad Prism 8.0 (GraphPad Software, Inc). The Brown-Forsythe and Bartlett's tests were performed to ensure homogeneity of variance and the

Shapiro-Wilk test was completed to assess normality. Statistical significance was evaluated using a two-way ANOVA with Bonferroni's multiple comparisons testing as indicated in the figure legends. For data that did not reflect a normal/Gaussian distribution, the Kruskal-Wallis test was utilized followed by Dunn's multiple comparisons test. Correlation analyses were evaluated using Pearson's correlation coefficient. For all analyses, a p value < 0.05 was considered statistically significant.

3. Results

3.1. Tau uptake in vitro

The microglia cultures showed the strongest interaction with tau at all 3 concentration (0.5, 5 and 50 ng/ml), while both the pericytes and smooth muscle cells demonstrated a dose-dependent capacity for tau uptake (Fig. 2). At the highest tau treatment concentration (50 ng/ml), the smooth muscle cells had essentially the same levels of intracellular tau as the microglia. In contrast, the astrocytes and brain endothelial cells showed a lower degree of tau uptake (at any concentration) as the tau levels in these cells were 3-times lower than that observed in the other cell types (pericytes, smooth muscle cells, and microglia) at 5 and 50 ng/ml and near the background level of detection. The rank order for the in vitro uptake of tau was microglia > smooth muscle cells > pericytes >> brain endothelia = astrocytes.

3.2. Cerebrovascular tau uptake ex vivo

Freshly isolated cerebrovessels from r-mTBI mice showed a progressive decline in tau uptake post-last injury, resulting in a statistically significant decrease at 6 (25%) and 12 months (30%) post-last injury compared to each respective r-sham cohort (Fig. 3A). Similarly, tau uptake was also significantly diminished (30% decrease) in cerebrovessels from mural cell-depleted PDGFR β (+/-) animals compared to age-matched wild-type littermates (Fig. 3B). Lastly, cerebrovessels from PSAPP animals demonstrated substantially less tau uptake (40% decrease) than age-matched wild-type littermates (Fig. 3C). Additionally, fluorescein-labeled A β (1-42) uptake was decreased (20%) in cerebrovessels from r-mTBI animals at 12 months post-last injury compared to r-sham mice (Fig. 4). Lastly, no difference in the cerebrovascular uptake of lucifer yellow dextran was observed between r-mTBI and r-sham animals at 12 months post-last injury (Fig. 4).

3.3. Mural cell marker expression in r-mTBI and transgenic animals

In the brain-injured animals, expression of the mural cell markers, α SMC-actin and PDGFR β , progressively decreased post-last injury in isolated r-mTBI cerebrovessels compared to r-sham animals. For α SMC-actin (Fig. 5A), a significant decrease was observed at both 6 and 12 months after the final injury (approximately 25% decrease for both compared to respective r-sham animals). For PDGFR β , expressions levels were significantly lower (approximately 30% decrease) at 12 months post-last injury compared to r-sham animals (Fig. 6A). Similarly, in the PDGFR β (+/-) animals (12 months of age), α SMC-actin in isolated cerebrovasculature was diminished (approximately 30%) compared to age-matched wild-type littermates, but this effect did not reach statistical significance (Fig. 5B). As anticipated, a substantial decrease in PDGFR β levels (approximately 40% reduction) was observed in the PDGFR β (+/-) animals compared to age-matched wild-type

littermates (Fig. 6B). Lastly, in the PSAPP mouse AD model (18 months of age), both α SMC-actin and PDGFR β were significantly reduced (approximately 30% decrease) in isolated cerebrovessels compared to age-matched wild-type littermates (Figs. 5C and 6C). In combining the tau uptake and mural cell expression datasets, we observed a strong correlation between cerebrovascular tau uptake and mural cell marker expression (α SMC-actin, $P=0.0195$; PDGFR β , $P=0.0335$) following repetitive trauma to the brain (Fig. 7).

3.4. Mural cell marker expression in human brain specimens

In isolated cerebrovasculature from human brain cortex, α SMC-actin levels in AD specimens were approximately half that observed in control specimens (Fig. 8A), and in the TBI specimens a reduction in α SMC-actin was also observed (approximately 25% compared to control brains), but this comparison was not statistically significant. While not quite as diminished as the AD group, α SMC-actin expression in the cerebrovasculature from the TBI-AD group was significantly lower than that found in control brains (Fig. 8A). For PDGFR β expression in isolated cerebrovessels, the levels in AD specimens were less than half that observed in control brains (Fig. 8B). In the TBI specimens, a reduction in PDGFR β expression was apparent (approximately 15% compared to control), but was not statistically significant. Lastly, in the AD-TBI group, PDGFR β levels were significantly reduced by 35% compared to control specimens (Fig. 8B).

3.5. Flow cytometry and immunophenotypic analysis of cerebrovascular mural cells and endothelia

The number of CD31 + ve endothelial cells and CD13 + ve mural cells in freshly isolated cerebrovasculature from r-sham and r-mTBI animals (6 months post-injury) were quantified and expressed as a percentage of the total number of gated events (Fig. 9). No significant difference was identified in the percentage of CD31 + ve endothelial cells (Fig. 9F) or CD13 + ve mural cells (Fig. 9G) when comparing r-sham and r-mTBI cerebrovessels.

3.6. Caveolin-1 expression in animal and human cerebrovasculature

Caveolin-1 expression was significantly decreased in isolated r-mTBI cerebrovessels compared to r-sham animals (35%) at 12 months post-last injury (Fig. 10). Similar reductions in cerebrovascular caveolin-1 expression were observed in both the PSAPP and PDGFR β (+/-) animals compared to their respective wild-type littermates (Fig. 10). With respect to the human brain specimens, cerebrovascular caveolin-1 levels were significantly reduced in the TBI brain specimens (40%), while nearly 2-times less caveolin-1 was detected in the AD cerebrovessels in relation to the control brain specimens (Fig. 11). The combination of TBI and AD had the lowest levels of cerebrovascular caveolin-1 demonstrating a 4-fold decrease when compared to the control brains (Fig. 11).

4. Discussion

Brain vascular mural cells are an essential component of the neurovascular unit, which couples neuronal activity to vascular function (ElAli et al., 2014) in regulating brain homeostasis (Hill et al., 2014). Specifically, mural cells perform a number of diverse functions including: cerebral blood flow regulation, blood-brain barrier (BBB) maintenance,

endothelial cell regulation and angiogenesis, and phagocytosis of extracellular solutes (Dalkara et al., 2011; Kolinko et al., 2018). As a result of their broad function and importance to cerebrovascular health, brain mural cells have been implicated in a variety of neurological pathologies (Hill et al., 2014; Dalkara et al., 2011). In the current studies, isolated cerebrovessels from human AD brain specimens and an AD mouse model (PSAPP) showed significant reductions in mural cell markers (PDGFR β and α SMC-actin) compared to age-matched human control brains and wild-type animals, respectively, consistent with prior reports of vascular mural cell disruptions in AD brains (Bourassa et al., 2020; Sagare et al., 2013; Sengillo et al., 2013).

As vascular mural cell perturbations are evident in AD and other neurodegenerative disorders (Winkler et al., 2013), we sought to interrogate the state of the mural cell population following trauma to the brain, particularly at more chronic timepoints post-injury, as such studies are currently lacking. In the acute phase post-injury, prior reporting showed numerous mural cell markers (including PDGFR β) were diminished in mouse cortical tissue up to 48 h following fluid percussion injury (Bhowmick et al., 2019). In this same post-injury window (48 h), at the ultrastructural level, it was found that a subset of pericytes associated with the microvasculature underwent a form of cellular degeneration, while another group of pericytes migrated from the endothelium in response to traumatic injury (Dore-Duffy et al., 2000). Thai and colleagues observed a rapid decline in PDGFR β within the first 12 h after injury, however by day 5 post-TBI, not only did these levels resolve but several mural cell markers were significantly elevated compared to control conditions (Zehendner et al., 2015). In our mouse model of r-mTBI, we observed an initial increase in α SMC-actin compared to r-sham animals (24 h post-injury), akin to that reported after TBI in prior studies (Dore-Duffy et al., 2011). However, as the post-injury time increased in our studies, both mural cell markers (PDGFR β and α SMC-actin) progressively devolved to levels comparable to that observed in the AD animal model. These findings were consistent with our previous observations using the same r-mTBI paradigm in an aged wild-type cohort (12 months of age) in which both PDGFR β and α SMC-actin were significantly decreased at 7 months post-injury, as determined through immunoblotting (Lynch et al., 2016). Furthermore, we interrogated these same markers in cerebrovessels isolated from human brain specimens and observed a decrease in both mural cell markers in the TBI brains compared to control specimens, though these analyses did not reach statistical significance. It is worth noting that only 1 of the 12 TBI specimens had at least one apolipoprotein E4 (apoE4) allele, which is a genetic risk factor for AD (Kim et al., 2009), while 11 of the 14 AD-TBI specimens were apoE4 positive, and is a likely reason the AD-TBI individuals converted to AD versus the TBI-only subjects. Additionally, a glaring difference between the human TBI specimens and the r-mTBI animal model is the number of brain injury exposures (1–2 TBI in the human specimens vs. 24 TBI in the mouse cohort). The r-mTBI paradigm intends to model the frequency of injuries experienced over the course of an entire career, such as contact sports athletes or military personnel. The more pronounced mural cell marker changes in the r-mTBI animal cohort versus the human TBI specimens could be the result of a higher injury frequency, though further investigation is certainly warranted.

While our findings revealed changes in key mural cell markers following head trauma, particularly in the chronic phase post-injury, what remains unclear is whether these

alterations are indicative of cellular degeneration or cellular loss. In human AD brains, PDGFR β levels were significantly reduced in the cortex and hippocampus (Sengillo et al., 2013), and both the mural cell number and vessel coverage was found to be reduced in mouse and human AD brains compared to control, using the mural cell-specific marker CD13 (Bourassa et al., 2020; Sagare et al., 2013; Sengillo et al., 2013). With respect to TBI, controlled cortical impact induced mural cell loss by 3 days after TBI in the perilesional cortex and ipsilateral hippocampal areas, as PDGFR β was found to be colocalized with several indicators of cell death (Choi et al., 2016), while a separate report showed CD13 levels were significantly diminished 48 h after fluid percussion injury (Bhowmick et al., 2019). In our studies, we performed flow cytometry to assess the state of the mural cell population after r-mTBI and found no change in the number of CD13+ cells between r-sham and r-mTBI cerebrovessels at 6 months post-injury. Furthermore, we recently reported no difference in mural cell vessel density between r-sham and r-mTBI animals (up to 9 months post-injury) based on CD13 vessel coverage using confocal microscopy (Lynch et al., 2020). Thus, while mural cell loss may occur acutely following brain trauma (Choi et al., 2016; Bhowmick et al., 2019), there does not appear to be an overt reduction in the number of mural cells in the chronic phase post-injury, but rather a progressive decline in key mural cell proteins (i.e., PDGFR β and α SMC-actin), which are expressed in both pericytes and smooth muscle cells (Alarcon-Martinez et al., 2018; Hellstrom et al., 1999; Skalli et al., 1989). It has been demonstrated that the PDGF pathway is tightly regulated and maintenance of the PDGFR β receptor is necessary for mural cell function and survival (Bell et al., 2010; Winkler et al., 2014). Similarly, alterations in smooth muscle-actin expression have been associated with changes in mural cell phenotype including cell contraction, migration, and survival (Ahmed and Warren, 2018). Smooth muscle-actin is an important component of mural cell contractility (Ahmed and Warren, 2018; Hamilton et al., 2010) and it has been suggested that the vasomotion wave initiated by contractile smooth muscle cells of cerebral arteries contributes to the clearance of fluid and solutes from the brain (Aldea et al., 2019). In fact, it was shown that reductions in arterial pulsatility decrease both the paravascular (Ilf et al., 2013) and perivascular (Carare et al., 2008) movement of solutes in the brain. As such, the chronic disruptions in PDGFR β and SMA we observed following repetitive head trauma may impact vasomotion during neurovascular coupling and the perivascular elimination of tau from the brain.

As described above, vascular mural cells contribute to the phagocytosis and clearance of a variety of extracellular molecules and are important mediators of solute disposition and accumulation in the brain (Winkler et al., 2014). Several studies have demonstrated the role of mural cells in the elimination of A β from the brain (Wildsmith et al., 2013; Alcendor, 2020; Kanekiyo et al., 2012; Kirabali et al., 2019; Ma et al., 2018), and we found A β uptake was diminished in r-mTBI cerebrovessels compared to the r-sham group. Comparatively, there has been little investigation into the interaction of tau with non-neuronal cells, particularly cells associated with the cerebrovasculature. We examined the association of tau with a panel of non-neuronal cells of the brain in vitro and found that brain vascular mural cells (pericytes and smooth muscle cells) interact with tau at a level near that observed with microglia cells, which are prominent phagocytic mediators of the brain and have been shown to degrade tau species (Majerova et al., 2014). Thus, vascular brain mural cells may be

involved in the uptake of tau, not unlike their role in the elimination of A β and other molecules from the brain. Moreover, disruption of these cells post-injury may lead to the presence of perivascular tau tangles, which is a pathological hallmark of human repetitive brain trauma (Stern et al., 2011; McKee et al., 2009). Similar to the A β study above, we investigated tau uptake in isolated cerebrovessels from r-mTBI mice and observed a progressive decline post-injury compared to r-sham cerebrovessels. The diminished cerebrovascular tau uptake at 12 months post-injury was similar to that observed in age-matched AD animals, both of which demonstrated a significantly reduced expression of cerebrovascular mural cell markers, as indicated above. As depicted in Fig. 7, we show a strong correlation between the expression of cerebrovascular mural cell markers and tau uptake following repetitive trauma to the brain. Moreover, the reduced cerebrovascular tau uptake in the current studies coincides with our prior work (using the same hTau mouse model and r-mTBI paradigm) where a significant increase in phosphorylated, oligomeric, and total tau levels was observed in the brain cortex post-injury compared to r-sham animals (Ojo et al., 2016). The general lack of perivascular tau in mouse TBI models compared to human TBI may be due to differences in brain anatomy (gyrencephalic vs lissencephalic) or the ratio of tau isoforms (3R vs 4R), but further investigation is needed to identify the nature of these species-related differences. Further evidence of a potential link between mural cell degeneration and tau disposition in the brain has been reported previously where an AD mouse model (which does not display tau pathology on its own) was crossed with transgenic mural cell-deficient mice and a significant elevation in tau pathology became evident in the cortex and hippocampus of the AD x mural cell-deficient crossed animals (Sagare et al., 2013). While our studies clearly show a progressive decline in markers for pericytes and smooth muscle cells following brain injury, our approaches do not identify the individual contributions of each cell type to tau uptake, outside of the *in vitro* tau uptake studies, nor do they differentiate the response of each cell type to head trauma. Despite these limitations, collectively the above studies suggest a role for vascular mural cells in the uptake of extracellular tau, and that disruption of these cells could potentiate tau pathology in the brain.

To understand the mechanics of tau internalization by vascular mural cells and the influence of brain trauma on these processes, we interrogated caveolin, an endocytic component found in mural cells that has been associated with the PDGF pathway (Sundberg et al., 2009). Coinciding with the reductions in cerebrovascular mural cell markers and tau uptake following r-mTBI, we observed a significant decrease in caveolin expression in the brain vasculature of the r-mTBI animals at 12 months post-injury, on par with that observed in mouse AD cerebrovessels. Moreover, similar reductions in caveolin-1 were observed in the human TBI and human AD cerebrovasculature. Interestingly, it has been shown that a loss of caveolin-1 accelerates aging and contributes to neurodegeneration (Head et al., 2010). In particular, mice with reduced caveolin-1 brain expression exhibit a number of TBI and AD pathological features including: increased beta-amyloid (Head et al., 2010), phosphorylated tau (Bonds et al., 2019; Head et al., 2010), and astrogliosis (Head et al., 2010), alongside decreased cerebrovascular volume (Head et al., 2010) and cognitive impairment (Bonds et al., 2019) compared to wild-type animals. Correspondingly, it was observed that caveolin-1 overexpression can reduce the extent of injury and enhance functional recovery after TBI

(Kellerhals et al., 2013). It is important to note that our cerebrovascular preparations likely contain brain endothelia and potentially astrocytes, which also express caveolin-1, and could contribute to the alterations in caveolin-1 we observed after r-mTBI and AD. However, any potential changes occurring in brain endothelia after TBI may not necessarily translate to tau uptake, as our in vitro findings suggest the interaction between tau and brain endothelia/astrocytes is minimal compared to vascular mural cells. Altogether, these findings suggest irregular PDGF signaling could impact the endocytic uptake of solutes via caveolin-1 and may explain the diminished tau uptake by the cerebrovasculature we observed in r-mTBI and AD mice.

Lastly, to more directly identify the link between mural cell disruption and tau internalization in brain vascular mural cells, we interrogated transgenic PDGFR β animals, which display reduced vascular mural cell coverage with age, as a result of genetic modifications to the PDGF receptor (Bell et al., 2010; Tallquist et al., 2003). Cerebrovessels isolated from 12 month-old PDGFR β (+/-) mice (same age as the 6 months post-last r-mTBI mice) showed significant reductions in PDGFR β and caveolin-1, in addition to diminished tau uptake compared to wild-type littermates, in line with our observations in the chronic phase following r-mTBI and the AD animals. Based on these findings, changes in the PDGF receptor causes the mural cell population in the brain to devolve post-injury, potentially reducing the elimination of extracellular tau by these cells, which may contribute to the elevation of tau species in the brain that occurs following head trauma. In addition to the elimination of extracellular solutes, mural cell degeneration may be an important factor in TBI etiology overall. The most compelling evidence for this concept may be the extensive overlap in pathophysiology between the r-mTBI mice and the transgenic mural cell-depleted PDGFR β animals. Both the r-mTBI and mural-cell depleted animals exhibit cerebrovascular abnormalities (Bell et al., 2010; DeWitt and Plough, 2003), neuroinflammation (Bell et al., 2010; Mouzon et al., 2014), white matter regression (Donovan et al., 2014; Montagne et al., 2018), and cognitive impairment (Bell et al., 2010; Mouzon et al., 2014). Importantly, it has been shown that mural cell degeneration precedes the neuroinflammatory response, neuronal decline, and cognitive dysfunction in transgenic PDGFR β animals (Bell et al., 2010). Similarly, in human AD microvessel extracts, it was found that reduced brain mural cell levels correlated with cognitive impairment and AD diagnosis (Bourassa et al., 2020). In our prior work using this r-mTBI mouse model, we observed a decline in cognitive performance at 1 month post-injury which progressively deteriorated at 3 and 6 months post-injury (Lynch et al., 2016; Lynch et al., 2020), in line with the mural cell degeneration we observed at these time points following r-mTBI in the current studies, though further work is needed to understand the potential correlation between brain mural cell changes and cognitive function. Collectively, these studies point toward mural cell disruption as a contributing factor in TBI pathogenesis and cognitive impairment.

5. Conclusion

A prominent pathological feature of repetitive head trauma in humans is the accumulation of hyperphosphorylated tau and the presence of neurofibrillary and perivascular tau tangles. Our findings indicate brain vascular mural cells interact with tau and may serve as a pathway for eliminating tau from extracellular brain fluids. Furthermore, human TBI brain specimens

and a mouse model of r-mTBI demonstrate a degeneration of mural cell markers in the chronic phase post-injury, coinciding with reduced cerebrovascular caveolin-1 expression and tau uptake, features consistent with those identified in transgenic mural cell-depleted PDGFR β (+/-) animals and an AD mouse model. Hence, as the mural cell population devolves in the aftermath of brain trauma or disease, cerebrovascular tau elimination is diminished, which may contribute to the brain deposition of tau species in TBI and other neurodegenerative diseases. Vascular mural cells have a prominent role in regulating brain function and their disruption following head trauma may be a critical driver of TBI pathophysiology and neurodegeneration.

Acknowledgements

The mural cell-depleted animals, PDGFR β (+/-), were kindly provided by Dr. Richard Daneman (University of California, San Diego, La Jolla, CA). We are grateful to the Banner Sun Health Research Institute Brain and Body Donation Program of Sun City, Arizona for the provision of human brain tissue. The Brain and Body Donation Program has been supported by the National Institute of Neurological Disorders and Stroke (U24 NS072026 National Brain and Tissue Resource for Parkinson's Disease and Related Disorders), the National Institute on Aging (P30 AG19610 Arizona Alzheimer's Disease Core Center), the Arizona Department of Health Services (contract 211002, Arizona Alzheimer's Research Center), the Arizona Biomedical Research Commission (contracts 4001, 0011, 05-901 and 1001 to the Arizona Parkinson's Disease Consortium) and the Michael J. Fox Foundation for Parkinson's Research.

Funding

This work was supported by the Department of Defense under award number W81XWH-16-1-0724-PRARP-CSRA. Opinions, interpretations, conclusions, and recommendations are those of the author and are not necessarily endorsed by the Department of Defense. This work was also supported by Merit Review award number I01BX003709 from the Department of Veterans Affairs (VA) Biomedical Laboratory Research and Development Program. The contents do not represent the views of the Department of Veterans Affairs or the United States Government. Dr. Bachmeier is a Research Scientist at the Bay Pines VA Healthcare System, Bay Pines, FL. Dr. Crawford is a Research Career Scientist at the James A. Haley Veterans Hospital, Tampa, FL. Finally, we would like to thank the Roskamp Institute for their generosity in helping to make this work possible.

References

- Ahmed S, Warren DT, 2018. Vascular smooth muscle cell contractile function and mechanotransduction. *Vessel Plus* 2 (36), 1–13. 10.20517/2574-1209.2018.51.
- Alarcon-Martinez L, Yilmaz-Ozcan S, Yemisci M, Schallek J, Kilic K, Can A, Di Polo A, Dalkara T, 2018. Capillary pericytes express alpha-smooth muscle actin, which requires prevention of filamentous-actin depolymerization for detection. *Elife* 7. 10.7554/eLife.34861.
- Alcendor DJ, 2020. Interactions between amyloid-beta proteins and human brain pericytes: implications for the pathobiology of Alzheimer's disease. *J. Clin. Med* 9 (5) 10.3390/jcm9051490.
- Aldea R, Weller RO, Wilcock DM, Carare RO, Richardson G, 2019. Cerebrovascular smooth muscle cells as the drivers of intramural periarterial drainage of the brain. *Front. Aging Neurosci* 11, 1. 10.3389/fnagi.2019.00001. [PubMed: 30740048]
- Andorfer C, Kress Y, Espinoza M, de Silva R, Tucker KL, Barde YA, Duff K, Davies P, 2003. Hyperphosphorylation and aggregation of tau in mice expressing normal human tau isoforms. *J. Neurochem* 86 (3), 582–590. [PubMed: 12859672]
- Bachmeier C, Paris D, Beaulieu-Abdelahad D, Mouzon B, Mullan M, Crawford F, 2013. A multifaceted role for apoE in the clearance of beta-amyloid across the blood-brain barrier. *Neurodegener. Dis* 11 (1), 13–21. [PubMed: 22572854]
- Bachmeier C, Shackleton B, Ojo J, Paris D, Mullan M, Crawford F, 2014. Apolipoprotein E isoform-specific effects on lipoprotein receptor processing. *NeuroMolecular Med.* 16 (4), 686–696. [PubMed: 25015123]

- Bell RD, Winkler EA, Sagare AP, Singh I, LaRue B, Deane R, Zlokovic BV, 2010. Pericytes control key neurovascular functions and neuronal phenotype in the adult brain and during brain aging. *Neuron* 68 (3), 409–427. [PubMed: 21040844]
- Bhowmick S, D’Mello V, Caruso D, Wallerstein A, Abdul-Muneer PM, 2019. Impairment of pericyte-endothelium crosstalk leads to blood-brain barrier dysfunction following traumatic brain injury. *Exp. Neurol* 317, 260–270. [PubMed: 30926390]
- Blaylock RL, Maroon J, 2011. Immunoexcitotoxicity as a central mechanism in chronic traumatic encephalopathy—a unifying hypothesis. *Surg. Neurol. Int* 2, 107. [PubMed: 21886880]
- Blyth BJ, Bazarian JJ, 2010. Traumatic alterations in consciousness: traumatic brain injury. *Emerg. Med. Clin. North Am* 28 (3), 571–594. 20709244. [PubMed: 20709244]
- Bonds JA, Shetti A, Bheri A, Chen Z, Disouky A, Tai L, Mao M, Head BP, Bonini MG, Haus JM, Minshall RD, Lazarov O, 2019. Depletion of caveolin-1 in type 2 diabetes model induces Alzheimer’s disease pathology precursors. *J Neurosci.* 39 (43), 8576–8583. 10.1523/JNEUROSCI.0730-19.2019. [PubMed: 31527120]
- Bourassa P, Tremblay C, Schneider JA, Bennett DA, Calon F, 2020. Brain mural cell loss in the parietal cortex in Alzheimer’s disease correlates with cognitive decline and TDP-43 pathology. *Neuropathol. Appl. Neurobiol* 10.1111/nan.12599.
- Carare RO, Bernardes-Silva M, Newman TA, Page AM, Nicoll JA, Perry VH, Weller RO, 2008. Solutes, but not cells, drain from the brain parenchyma along basement membranes of capillaries and arteries: significance for cerebral amyloid angiopathy and neuroimmunology. *Neuropathol. Appl. Neurobiol* 34 (2), 131–144. [PubMed: 18208483]
- Chai X, Dage JL, Citron M, 2012. Constitutive secretion of tau protein by an unconventional mechanism. *Neurobiol. Dis.* 48 (3), 356–366. [PubMed: 22668776]
- Choi YK, Maki T, Mandeville ET, Koh SH, Hayakawa K, Arai K, Kim YM, Whalen MJ, Xing C, Wang X, Kim KW, Lo EH, 2016. Dual effects of carbon monoxide on pericytes and neurogenesis in traumatic brain injury. *Nat. Med* 22 (11), 1335–1341. [PubMed: 27668935]
- Crouch EE, Doetsch F, 2018. FACS isolation of endothelial cells and pericytes from mouse brain microregions. *Nat. Protoc* 13 (4), 738–751. 10.1038/nprot.2017.158. [PubMed: 29565899]
- Dalkara T, Gursoy-Ozdemir Y, Yemisci M, 2011. Brain microvascular pericytes in health and disease. *Acta Neuropathol.* 122 (1), 1–9. [PubMed: 21656168]
- DeWitt DS, Prough DS, 2003. Traumatic cerebral vascular injury: the effects of concussive brain injury on the cerebral vasculature. *J. Neurotrauma* 20 (9), 795–825. [PubMed: 14577860]
- Donovan V, Kim C, Anugerah AK, Coats JS, Oyoyo U, Pardo AC, Obenaus A, 2014. Repeated mild traumatic brain injury results in long-term white-matter disruption. *J. Cereb. Blood Flow Metab* 34 (4), 715–723. [PubMed: 24473478]
- Dore-Duffy P, Owen C, Balabanov R, Murphy S, Beaumont T, Rafols JA, 2000. Pericyte migration from the vascular wall in response to traumatic brain injury. *Microvasc. Res* 60 (1), 55–69. 10.1006/mvre.2000.2244. [PubMed: 10873515]
- Dore-Duffy P, Wang S, Mehedi A, Katyshev V, Cleary K, Tapper A, Reynolds C, Ding Y, Zhan P, Rafols J, Kreipke CW, 2011. Pericyte-mediated vasoconstriction underlies TBI-induced hypoperfusion. *Neurol. Res* 33 (2), 176–186. 10.1179/016164111X12881719352372. [PubMed: 21801592]
- ElAli A, Theriault P, Rivest S, 2014. The role of pericytes in neurovascular unit remodeling in brain disorders. *Int. J. Mol. Sci* 15 (4), 6453–6474. [PubMed: 24743889]
- Goldstein LE, Fisher AM, Tagge CA, Zhang XL, Velisek L, Sullivan JA, Upreti C, Kracht JM, Ericsson M, Wojnarowicz MW, Goletiani CJ, Maglakelidze GM, Casey N, Moncaster JA, Minaeva O, Moir RD, Nowinski CJ, Stern RA, Cantu RC, Geiling J, Blusztajn JK, Wolozin BL, Ikezu T, Stein TD, Budson AE, Kowall NW, Chargin D, Sharon A, Saman S, Hall GF, Moss WC, Cleveland RO, Tanzi RE, Stanton PK, McKee AC, 2012. Chronic traumatic encephalopathy in blast-exposed military veterans and a blast neurotrauma mouse model. *Sci. Transl. Med* 4 (134), 134ra60.
- Hamilton NB, Attwell D, Hall CN, 2010. Pericyte-mediated regulation of capillary diameter: a component of neurovascular coupling in health and disease. *Front. Neuroenerget* 2. 10.3389/ftene.2010.00005.

- Head BP, Peart JN, Panneerselvam M, Yokoyama T, Pearn ML, Niesman IR, Bonds JA, Schilling JM, Miyahara A, Headrick J, Ali SS, Roth DM, Patel PM, Patel HH, 2010. Loss of caveolin-1 accelerates neurodegeneration and aging. *PLoS One* 5 (12), e15697. [PubMed: 21203469]
- Hellstrom M, Kalen M, Lindahl P, Abramsson A, Betsholtz C, 1999. Role of PDGF-B and PDGFR-beta in recruitment of vascular smooth muscle cells and pericytes during embryonic blood vessel formation in the mouse. *Development* 126 (14), 3047–3055. [PubMed: 10375497]
- Hill J, Rom S, Ramirez SH, Persidsky Y, 2014. Emerging roles of pericytes in the regulation of the neurovascular unit in health and disease. *J. NeuroImmune Pharmacol* 9 (5), 591–605. [PubMed: 25119834]
- Holcomb L, Gordon MN, McGowan E, Yu X, Benkovic S, Jantzen P, Wright K, Saad I, Mueller R, Morgan D, Sanders S, Zehr C, O'Campo K, Hardy J, Prada CM, Eckman C, Younkin S, Hsiao K, Duff K, 1998. Accelerated Alzheimer-type phenotype in transgenic mice carrying both mutant amyloid precursor protein and presenilin 1 transgenes. *Nat. Med* 4 (1), 97–100. 10.1038/nm0198-097. [PubMed: 9427614]
- Huber BR, Meabon JS, Martin TJ, Mourad PD, Bennett R, Kraemer BC, Cernak I, Petrie EC, Emery MJ, Swenson ER, Mayer C, Mehic E, Peskind ER, Cook DG, 2013. Blast exposure causes early and persistent aberrant phospho-and cleaved-tau expression in a murine model of mild blast-induced traumatic brain injury. *J. Alzheimers Dis* 37 (2), 309–323. [PubMed: 23948882]
- Iliff JJ, Wang M, Zeppenfeld DM, Venkataraman A, Plog BA, Liao Y, Deane R, Nedergaard M, 2013. Cerebral arterial pulsation drives paravascular CSF-interstitial fluid exchange in the murine brain. *J. Neurosci* 33 (46), 18190–18199. [PubMed: 24227727]
- Iliff JJ, Chen MJ, Plog BA, Zeppenfeld DM, Soltero M, Yang L, Singh I, Deane R, Nedergaard M, 2014. Impairment of glymphatic pathway function promotes tau pathology after traumatic brain injury. *J. Neurosci* 34 (49), 16180–16193. [PubMed: 25471560]
- Kanekiyo T, Liu CC, Shinohara M, Li J, Bu G, 2012. LRP1 in brain vascular smooth muscle cells mediates local clearance of Alzheimer's amyloid-beta. *J. Neurosci* 32 (46), 16458–16465. 10.1523/JNEUROSCI.3987-12.2012. [PubMed: 23152628]
- Karch CM, Jeng AT, Goate AM, 2012. Extracellular Tau levels are influenced by variability in Tau that is associated with tauopathies. *J. Biol. Chem* 287 (51), 42751–42762. [PubMed: 23105105]
- Kellerhals S, Niesman I, Schilling J, Kleschevnikov A, Lysenko L, Roth D, Patel H, Patel P, Head B, 2013. Caveolin-1 overexpression repairs neuronal degradation in the setting of traumatic brain injury. *FASEB J.* 27, 693.10.
- Kim J, Basak JM, Holtzman DM, 2009. The role of apolipoprotein E in Alzheimer's disease. *Neuron* 63 (3), 287–303. 10.1016/j.neuron.2009.06.026. [PubMed: 19679070]
- Kirabali T, Rigotti S, Siccoli A, Liebsch F, Shobo A, Hock C, Nitsch RM, Multhaup G, Kulic L, 2019. The amyloid-beta degradation intermediate Abeta34 is pericyte-associated and reduced in brain capillaries of patients with Alzheimer's disease. *Acta Neuropathol. Commun* 7 (1), 194. 10.1186/s40478-019-0846-8. [PubMed: 31796114]
- Kolinko Y, Kralickova M, Tonar Z, 2018. The impact of pericytes on the brain and approaches for their morphological analysis. *J. Chem. Neuroanat* 91, 35–45. [PubMed: 29678665]
- Le MN, Kim W, Lee S, McKee AC, Hall GF, 2012. Multiple mechanisms of extracellular tau spreading in a non-transgenic tauopathy model. *Am. J. Neurodegener. Dis* 1 (3), 316–333. [PubMed: 23383401]
- Lynch CE, Crynen G, Ferguson S, Mouzon B, Paris D, Ojo J, Leary P, Crawford F, Bachmeier C, 2016. Chronic cerebrovascular abnormalities in a mouse model of repetitive mild traumatic brain injury. *Brain Inj.* 30 (12), 1414–1427. [PubMed: 27834539]
- Lynch CE, Eisenbaum M, Algamil M, Balbi M, Ferguson S, Mouzon B, Saltiel N, Ojo J, Diaz-Arrastia R, Mullan M, Crawford F, Bachmeier C, 2020. Impairment of cerebrovascular reactivity in response to hypercapnic challenge in a mouse model of repetitive mild traumatic brain injury. *J. Cereb. Blood Flow Metab* 10.1177/0271678x20954015.
- Ma Q, Zhao Z, Sagare AP, Wu Y, Wang M, Owens NC, Verghese PB, Herz J, Holtzman DM, Zlokovic BV, 2018. Blood-brain barrier-associated pericytes internalize and clear aggregated amyloid-beta42 by LRP1-dependent apolipoprotein E isoform-specific mechanism. *Mol. Neurodegener* 13 (1), 57. 10.1186/s13024-018-0286-0. [PubMed: 30340601]

- Magnoni S, Esparza TJ, Conte V, Carbonara M, Carrabba G, Holtzman DM, Zipfel GJ, Stocchetti N, Brody DL, 2012. Tau elevations in the brain extracellular space correlate with reduced amyloid-beta levels and predict adverse clinical outcomes after severe traumatic brain injury. *Brain* 135 (Pt 4), 1268–1280. [PubMed: 22116192]
- Majerova P, Zilkova M, Kazmerova Z, Kovac A, Paholikova K, Kovacech B, Zilka N, Novak M, 2014. Microglia display modest phagocytic capacity for extracellular tau oligomers. *J. Neuroinflammation* 11 (1), 161. [PubMed: 25217135]
- Marklund N, Blennow K, Zetterberg H, Ronne-Engstrom E, Enblad P, Hillered L, 2009. Monitoring of brain interstitial total tau and beta amyloid proteins by microdialysis in patients with traumatic brain injury. *J. Neurosurg* 110 (6), 1227–1237. [PubMed: 19216653]
- McKee AC, Cantu RC, Nowinski CJ, Hedley-Whyte ET, Gavett BE, Budson AE, Santini VE, Lee HS, Kubilus CA, Stern RA, 2009. Chronic traumatic encephalopathy in athletes: progressive tauopathy after repetitive head injury. *J. Neuropathol. Exp. Neurol* 68 (7), 709–735. 19535999. [PubMed: 19535999]
- Medina M, Avila J, 2014. The role of extracellular Tau in the spreading of neurofibrillary pathology. *Front. Cell. Neurosci* 8, 113. [PubMed: 24795568]
- Michel CH, Kumar S, Pinotsi D, Tunnacliffe A, St George-Hyslop P, Mandelkow E, Mandelkow EM, Kaminski CF, Kaminski Schierle GS, 2013. Extracellular monomeric tau protein is sufficient to initiate the spread of tau protein pathology. *J. Biol. Chem* 289 (2), 956–967. [PubMed: 24235150]
- Montagne A, Nikolakopoulou AM, Zhao Z, Sagare AP, Si G, Lazic D, Barnes SR, Daianu M, Ramanathan A, Go A, Lawson EJ, Wang Y, Mack WJ, Thompson PM, Schneider JA, Varkey J, Langen R, Mullins E, Jacobs RE, Zlokovic BV, 2018. Pericyte degeneration causes white matter dysfunction in the mouse central nervous system. *Nat. Med* 24 (3), 326–337. [PubMed: 29400711]
- Mouzon B, Chaytow H, Crynen G, Bachmeier C, Stewart J, Mullan M, Stewart W, Crawford F, 2012. Repetitive mild traumatic brain injury in a mouse model produces learning and memory deficits accompanied by histological changes. *J. Neurotrauma* 29 (18), 2761–2773. [PubMed: 22900595]
- Mouzon BC, Bachmeier C, Ferro A, Ojo JO, Crynen G, Acker CM, Davies P, Mullan M, Stewart W, Crawford F, 2014. Chronic neuropathological and neurobehavioral changes in a repetitive mild traumatic brain injury model. *Ann. Neurol* 75 (2), 241–254. [PubMed: 24243523]
- Ojo JO, Mouzon B, Greenberg MB, Bachmeier C, Mullan M, Crawford F, 2013. Repetitive mild traumatic brain injury augments tau pathology and glial activation in aged hTau mice. *J. Neuropathol. Exp. Neurol* 72 (2), 137–151. [PubMed: 23334597]
- Ojo JO, Mouzon B, Algamal M, Leary P, Lynch C, Abdullah L, Evans J, Mullan M, Bachmeier C, Stewart W, Crawford F, 2016. Chronic repetitive mild traumatic brain injury results in reduced cerebral blood flow, axonal injury, gliosis, and increased T-tau and tau oligomers. *J. Neuropathol. Exp. Neurol* 75 (7), 636–655. [PubMed: 27251042]
- Omalu B, Bailes J, Hamilton RL, Kamboh MI, Hammers J, Case M, Fitzsimmons R, 2011. Emerging histomorphologic phenotypes of chronic traumatic encephalopathy in American athletes. *Neurosurgery* 69 (1), 173–183. [PubMed: 21358359]
- Ost M, Nylen K, Csajbok L, Ohrfelt AO, Tullberg M, Wikkelso C, Nellgard P, Rosengren L, Blennow K, Nellgard B, 2006. Initial CSF total tau correlates with 1-year outcome in patients with traumatic brain injury. *Neurology* 67 (9), 1600–1604. [PubMed: 17101890]
- Petraglia AL, Plog BA, Dayawansa S, Dashnaw ML, Czerniecka K, Walker CT, Chen M, Hyrien O, Iliff JJ, Deane R, Huang JH, Nedergaard M, 2014. The pathophysiology underlying repetitive mild traumatic brain injury in a novel mouse model of chronic traumatic encephalopathy. *Surg. Neurol. Int* 5, 184. [PubMed: 25593768]
- Sagare AP, Bell RD, Zhao Z, Ma Q, Winkler EA, Ramanathan A, Zlokovic BV, 2013. Pericyte loss influences Alzheimer-like neurodegeneration in mice. *Nat. Commun* 4, 2932. [PubMed: 24336108]
- Sengillo JD, Winkler EA, Walker CT, Sullivan JS, Johnson M, Zlokovic BV, 2013. Deficiency in mural vascular cells coincides with blood-brain barrier disruption in Alzheimer's disease. *Brain Pathol.* 23 (3), 303–310. [PubMed: 23126372]
- Skalli O, Pelte MF, Pecllet MC, Gabbiani G, Gugliotta P, Bussolati G, Ravazzola M, Orci L, 1989. Alpha-smooth muscle actin, a differentiation marker of smooth muscle cells, is present in

- microfilamentous bundles of pericytes. *J. Histochem. Cytochem* 37 (3), 315–321. [PubMed: 2918221]
- Stern RA, Riley DO, Daneshvar DH, Nowinski CJ, Cantu RC, McKee AC, 2011. Long-term consequences of repetitive brain trauma: chronic traumatic encephalopathy. *PM R.* 3 (10 Suppl 2), S460–S467. [PubMed: 22035690]
- Sundberg C, Friman T, Hecht LE, Kuhl C, Solomon KR, 2009. Two different PDGF beta-receptor cohorts in human pericytes mediate distinct biological endpoints. *Am. J. Pathol* 175 (1), 171–189. [PubMed: 19497991]
- Tallquist MD, French WJ, Soriano P, 2003. Additive effects of PDGF receptor beta signaling pathways in vascular smooth muscle cell development. *PLoS Biol.* 1 (2), E52. [PubMed: 14624252]
- Tsitsopoulos PP, Marklund N, 2013. Amyloid-beta peptides and tau protein as biomarkers in cerebrospinal and interstitial fluid following traumatic brain injury: a review of experimental and clinical studies. *Front. Neurol* 4, 79. 23805125. [PubMed: 23805125]
- Wildsmith KR, Holley M, Savage JC, Skerrett R, Landreth GE, 2013. Evidence for impaired amyloid beta clearance in Alzheimer's disease. *Alzheimers Res. Ther* 5 (4), 33. [PubMed: 23849219]
- Winkler EA, Sengillo JD, Sullivan JS, Henkel JS, Appel SH, Zlokovic BV, 2013. Blood-spinal cord barrier breakdown and pericyte reductions in amyotrophic lateral sclerosis. *Acta Neuropathol.* 125 (1), 111–120. [PubMed: 22941226]
- Winkler EA, Sagare AP, Zlokovic BV, 2014. The pericyte: a forgotten cell type with important implications for Alzheimer's disease? *Brain Pathol.* 24 (4), 371–386. [PubMed: 24946075]
- Zehendner CM, Sebastiani A, Hugonnet A, Bischoff F, Luhmann HJ, Thal SC, 2015. Traumatic brain injury results in rapid pericyte loss followed by reactive pericytosis in the cerebral cortex. *Sci. Rep* 5, 13497. [PubMed: 26333872]
- Zhang J, Teng Z, Song Y, Hu M, Chen C, 2014. Inhibition of monoacylglycerol lipase prevents chronic traumatic encephalopathy-like neuropathology in a mouse model of repetitive mild closed head injury. *J. Cereb. Blood Flow Metab* 35 (3), 443–453. [PubMed: 25492114]

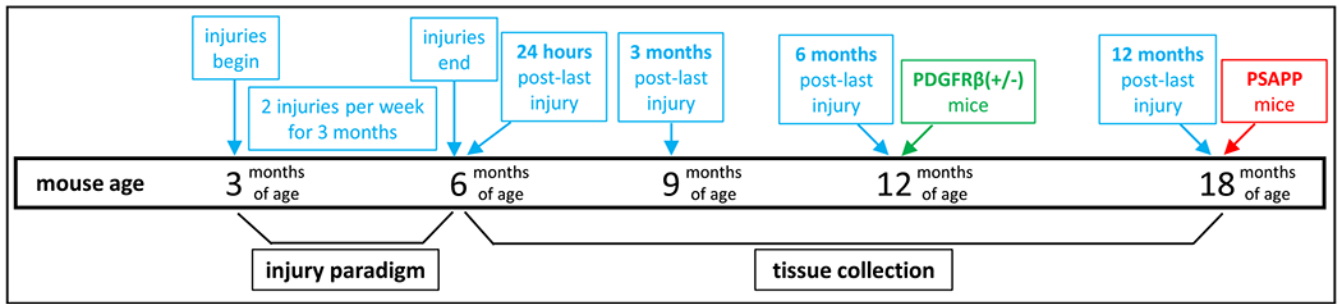


Fig. 1.

Timeline of the brain injury paradigm and tissue collection for the mouse studies. Human tau (hTau) mice at 3 months of age received 2 injuries per week for 3 months. As a control, sham animals did not receive any brain injuries, but were exposed to anesthesia for the same length of time as the injured mice and under the same paradigm (2 exposures per week for 3 months). Mice were euthanized and tissue was collected at 24 h, 3 months, 6 months, and 12 months after the final brain injury or anesthesia exposure (blue boxes). Moreover, transgenic mural cell-depleted animals, PDGFR β (+/-) (green box), and a mouse model of Alzheimer's disease, PSAPP (red box), were euthanized and tissue collected at 12 months and 18 months of age, respectively. Of note, neither the PDGFR β (+/-) nor PSAPP animals were administered any brain injuries. (For interpretation of the references to colour in this figure legend, the reader is referred to the web version of this article.)

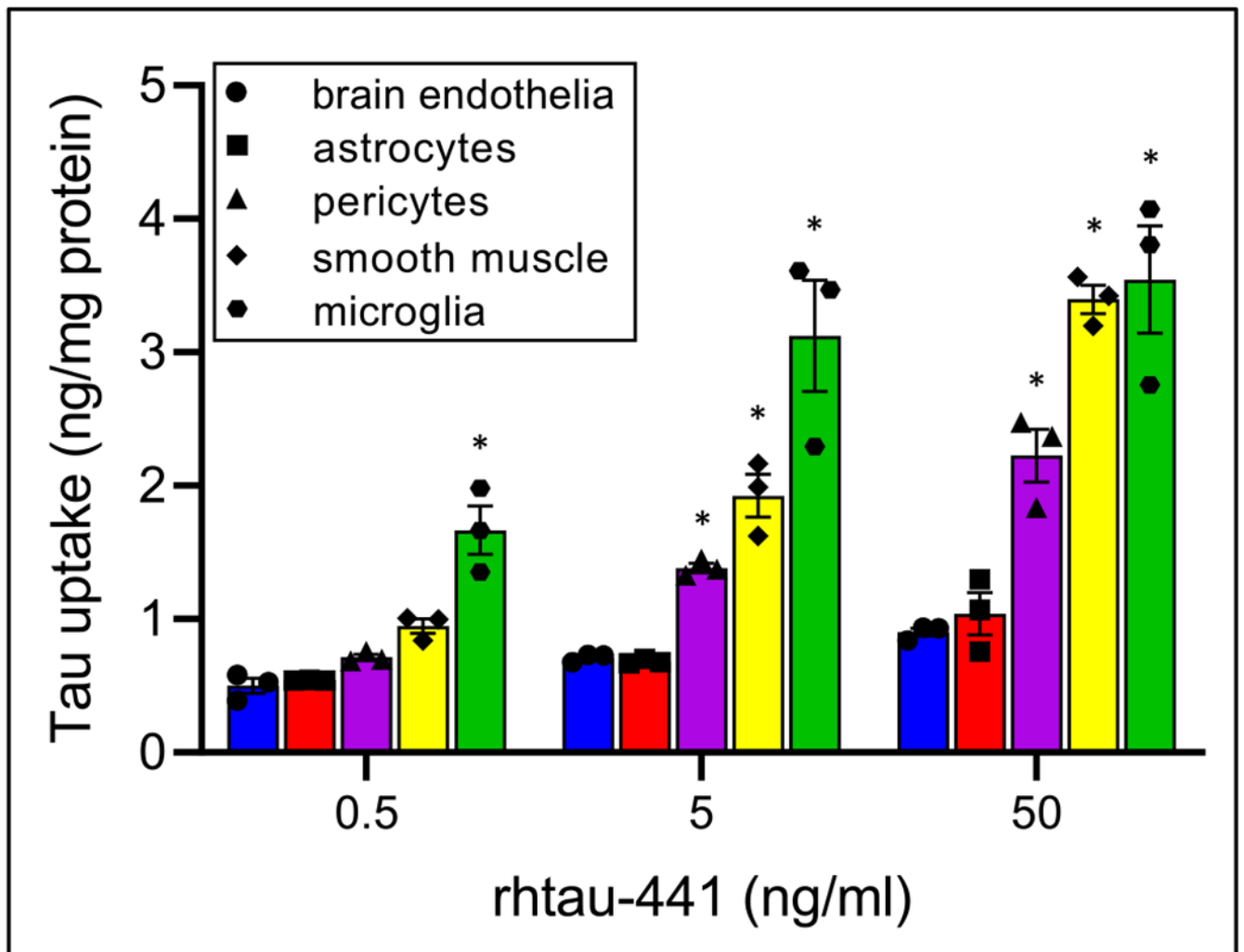
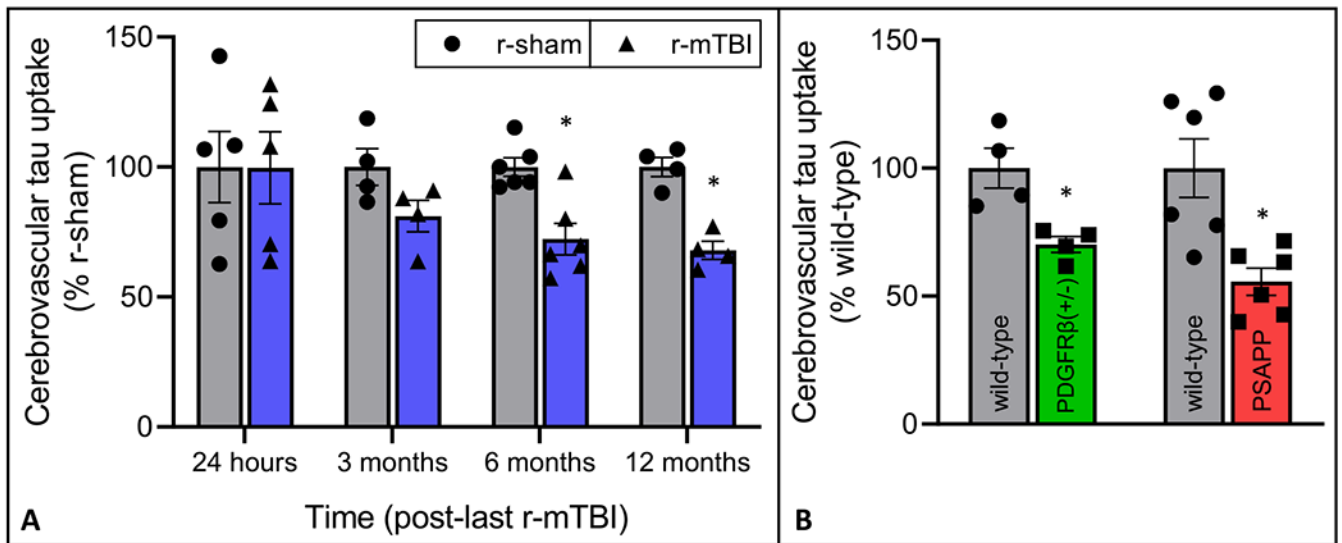


Fig. 2. Tau uptake in human non-neuronal brain cells. Cells were exposed to various concentrations (0.5, 5, and 50 ng/ml) of full length recombinant human tau (rhtau-441) for 1 h at 37 °C. Lysates were analyzed for tau content by ELISA and normalized to total protein using the BCA assay. Values represent mean \pm SEM ($n = 3$) and are expressed as ng of tau per mg of total protein. * $P < 0.05$ compared to brain endothelia as determined by two-way ANOVA and Bonferroni's multiple comparisons test.

**Fig. 3.**

Tau uptake in freshly isolated cerebrovasculature from (A) r-mTBI mice (24 h, 3 months, 6 months, and 12 months post-last injury), and (B) PDGFR β (+/-) mice, PSAPP mice, and respective wild-type littermates. Cerebrovessels were exposed to 5 ng/ml recombinant human tau (rhtau-441) for 1 h at 37 °C. Lysates were analyzed for tau content by ELISA and normalized to total protein using the BCA assay. Values represent mean \pm SEM and are expressed as a percentage of each respective r-sham or wild-type littermate. The sample sizes for the r-sham and r-mTBI groups were the same for each timepoint: 24 h ($n = 5$), 3 months ($n = 4$), 6 months ($n = 6$), and 12 months ($n = 4$). PDGFR β (+/-) and wild-type littermates ($n = 4$ each) and PSAPP and wild-type littermates ($n = 6$ each). * $P < 0.05$ compared to each respective r-sham or wild-type littermate as determined by two-way ANOVA and Bonferroni's multiple comparisons test.

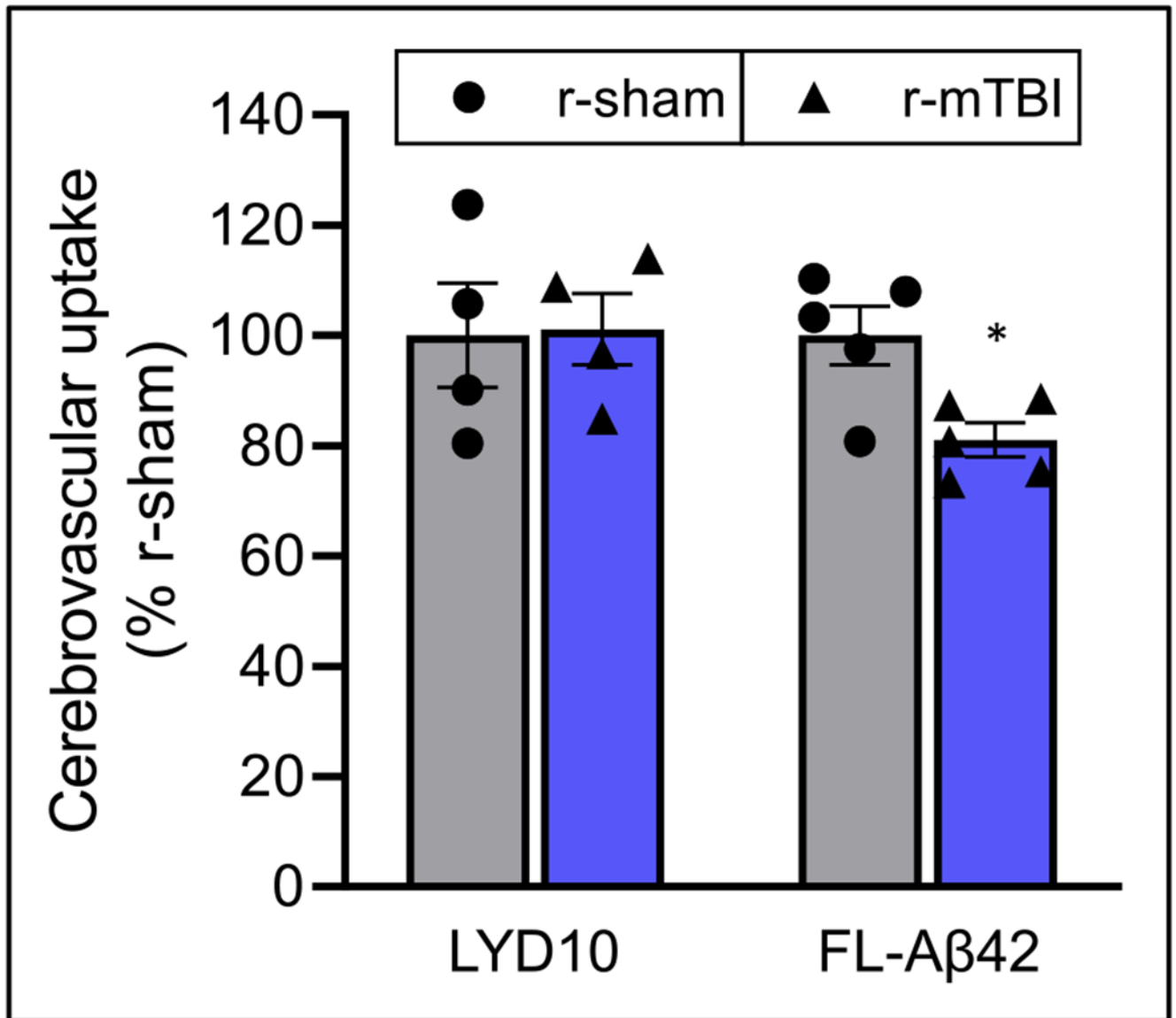


Fig. 4. Solute uptake in freshly isolated cerebrovasculature from r-mTBI mice at 12 months post-last injury. Cerebrovessels were exposed to lucifer yellow dextran (10 μ M) or fluorescein-labeled A β 1-42 (2 μ M) for 1 h at 37 $^{\circ}$ C. Lysates were analyzed for fluorescence and normalized to total protein using the BCA assay. Values represent mean \pm SEM and are expressed as a percentage of each respective r-sham group. The sample sizes for the r-sham and r-mTBI groups were the same for each probe: lucifer yellow dextran (n = 4), fluorescein-labeled A β 1-42 (n = 5). *P < 0.05 compared to each respective r-sham as determined by two-way ANOVA and Bonferroni's multiple comparisons test.

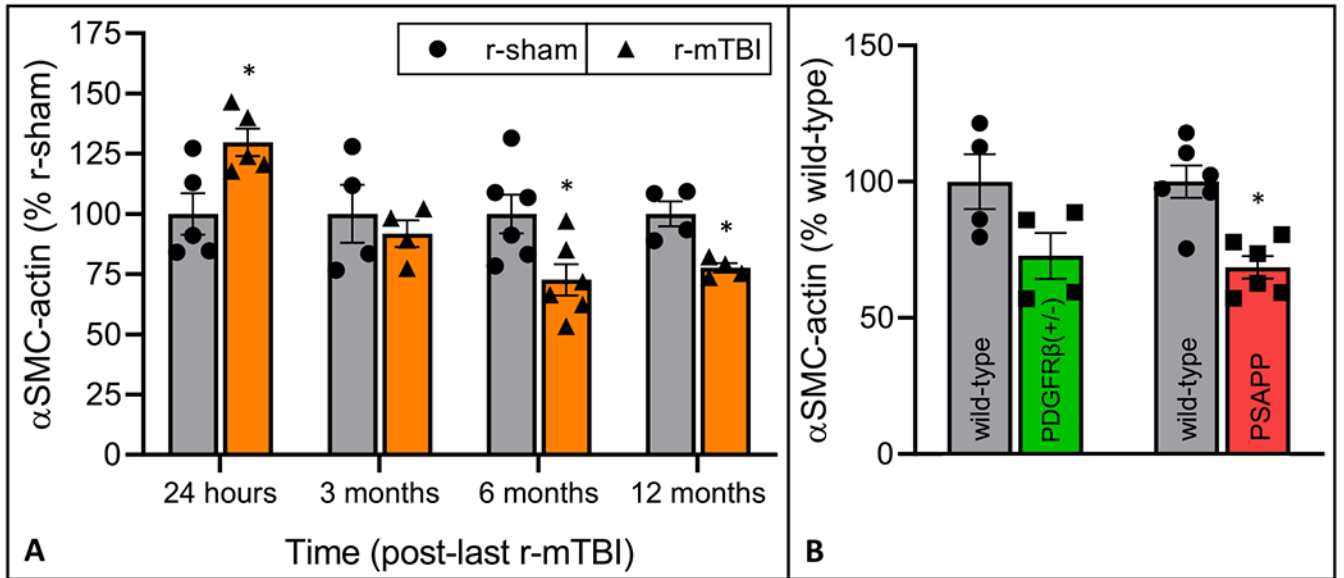


Fig. 5. Mural cell marker expression (α SMC-actin) in freshly isolated cerebrovasculature from (A) r-mTBI mice (24 h, 3 months, 6 months, and 12 months post-last injury), and (B) PDGFR β (+/-) mice, PSAPP mice, and respective wild-type littermates. Lysates were analyzed for α SMC-actin by ELISA and normalized to total protein using the BCA assay. Values represent mean \pm SEM and are expressed as a percentage of each respective r-sham or wild-type littermate. The sample sizes for the r-sham and r-mTBI groups were the same for each timepoint: 24 h (n = 5), 3 months (n = 4), 6 months (n = 6), and 12 months (n = 4). PDGFR β (+/-) and wild-type littermates (n = 4 each) and PSAPP and wild-type littermates (n = 6 each). *P < 0.05 compared to each respective r-sham or wild-type littermate as determined by two-way ANOVA and Bonferroni's multiple comparisons test.

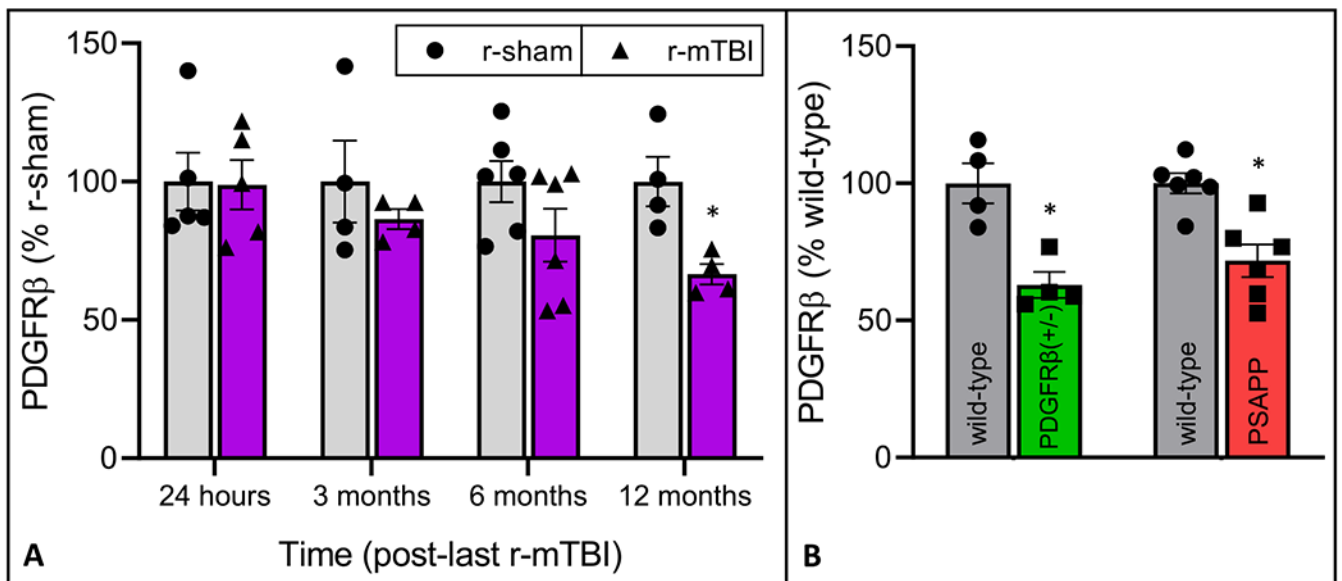


Fig. 6. Mural cell marker expression (PDGFR β) in freshly isolated cerebrovasculature from (A) r-mTBI mice (24 h, 3 months, 6 months, and 12 months post-last injury), and (B) PDGFR β (+/-) mice, PSAPP mice, and respective wild-type littermates. Lysates were analyzed for PDGFR β by ELISA and normalized to total protein using the BCA assay. Values represent mean \pm SEM and are expressed as a percentage of each respective r-sham or wild-type littermate. The sample sizes for the r-sham and r-mTBI groups were the same for each timepoint: 24 h (n = 5), 3 months (n = 4), 6 months (n = 6), and 12 months (n = 4). PDGFR β (+/-) and wild-type littermates (n = 4 each) and PSAPP and wild-type littermates (n = 6 each). *P < 0.05 compared to each respective r-sham or wild-type littermate as determined by two-way ANOVA and Bonferroni's multiple comparisons test.

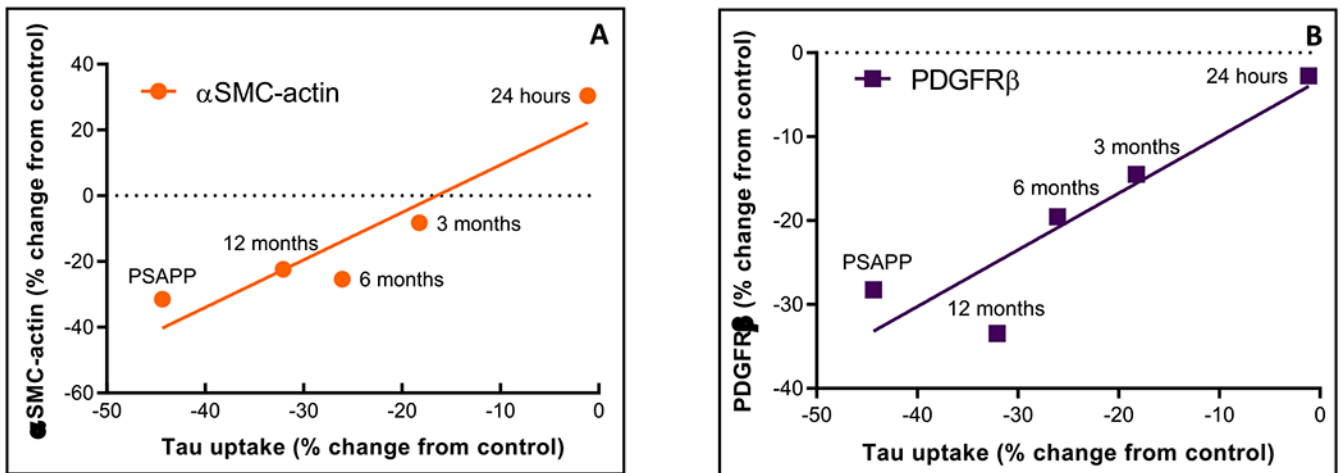


Fig. 7.

Correlation between mural cell expression and tau uptake in cerebrovessels isolated from r-mTBI (24 h, 3 months, 6 months, and 12 months post-last injury) and PSAPP mice.

Cerebrovascular expression of (A) α SMC-actin, and (B) PDGFR β was plotted versus tau uptake (α SMC-actin, $r = 0.93$; PDGFR β , $r = 0.91$). Values represent the mean % change from each respective control (r-sham or wild-type littermates). α SMC-actin ($P = 0.0195$) and PDGFR β ($P = 0.0335$) as determined by a two-tailed Pearson correlation.

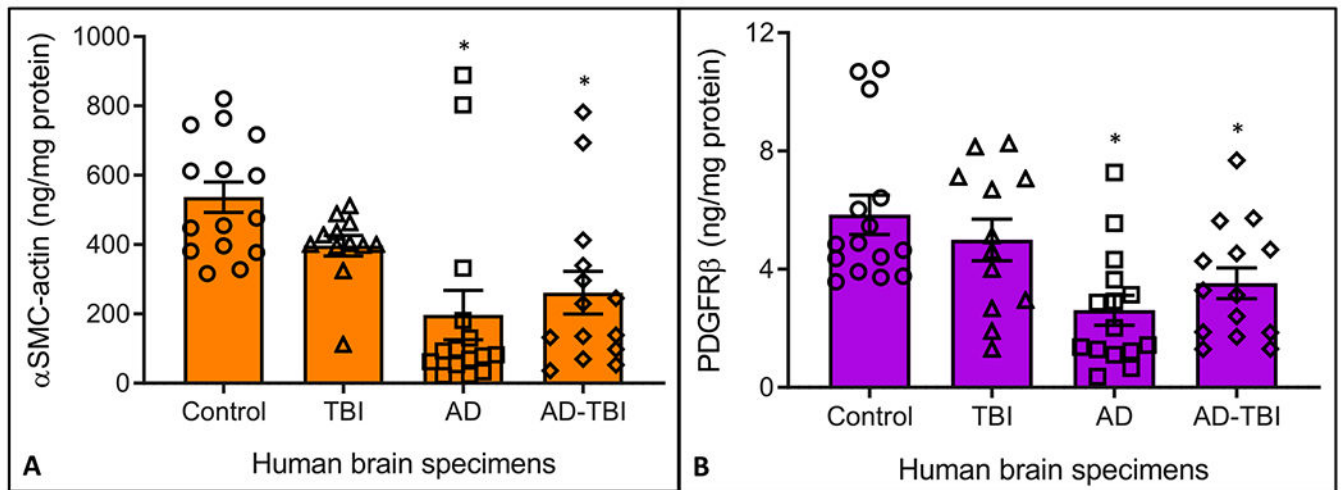
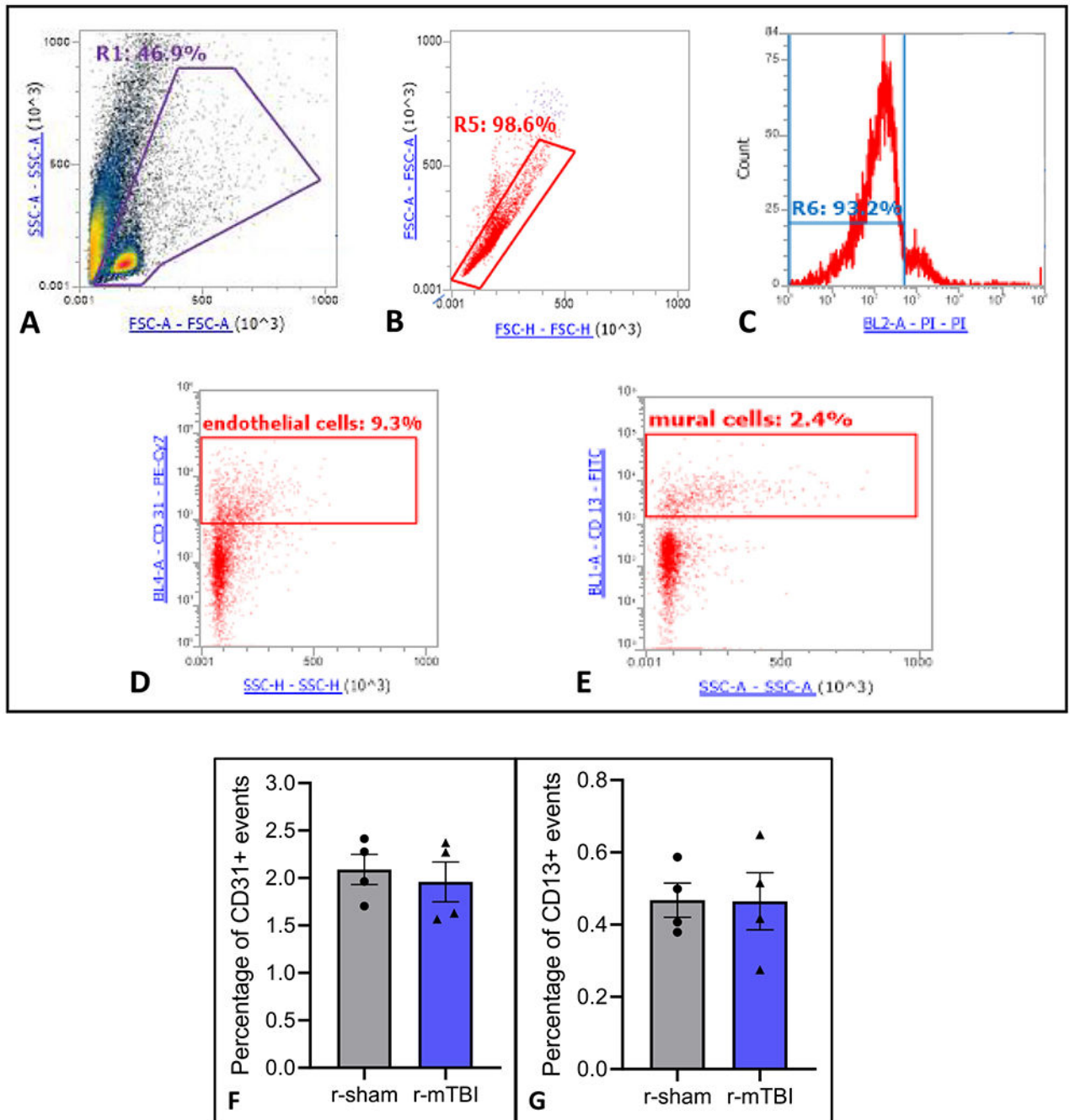


Fig. 8. Mural cell marker expression in cerebrovasculature isolated from human brain cortex derived from, 1) non-demented control subjects (no history of TBI or AD diagnosis), 2) TBI, 3) AD, and 4) TBI and AD. Lysates were analyzed for (A) α SMC-actin, and (B) PDGFR β by ELISA and normalized to total protein using the BCA assay. Values represent mean \pm SEM and are expressed as ng per mg of total protein. Control ($n = 15$), TBI ($n = 12$), AD ($n = 15$), TBI-AD ($n = 14$). * $P < 0.05$ compared to control as determined by the Kruskal-Wallis test followed by Dunn's multiple comparisons test.

**Fig. 9.**

Flow cytometry analysis of brain endothelia and mural cells in freshly isolated cerebrovasculature from r-sham and r-mTBI mice at 6 months post-last injury. The scatter plot diagrams represent the gating strategy used during the identification and analysis of CD31 + ve endothelial cells and CD13 + ve mural cells. Cellular debris was excluded through gating based on (A) particle size (forward scatter area FSC-A) and particle complexity (side scatter area SSC-A). Gating based on (B) FSCH (H- height) and FSC-A (A- area scaling) selected for single cell populations, while live cells were identified through

(C) negative propidium iodide staining. The resulting sample populations were gated based on (D) positive expression of PE-Cy7 indicating CD31 + ve endothelial cells, and (E) positive expression of fluorescein isothiocyanate (FITC) indicating CD13 + ve mural cells. The percentages refer to the proportion of endothelia or mural cells in relation to the previous parent gate. Figs. F and G represent the percentage of CD31 + ve endothelial cells and CD13 + ve mural cells, respectively, in relation to the total number of gated events in r-sham and r-mTBI cerebrovessels. Values represent mean \pm SEM (n = 4). *P < 0.05 compared to r-sham as determined by a one-way ANOVA followed by post-hoc test correction for false discovery rate using the Bonferroni correction.

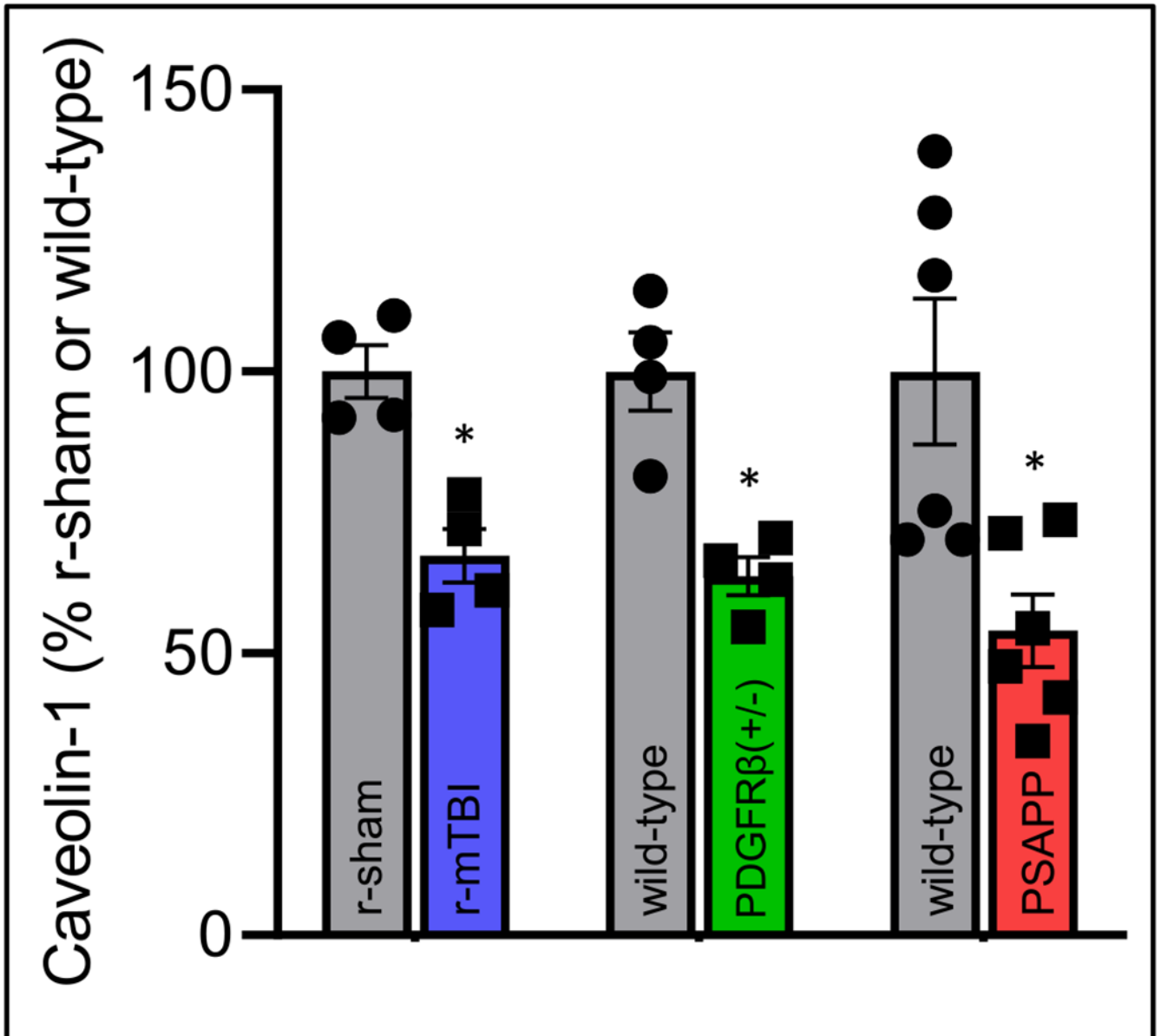


Fig. 10.

Caveolin-1 expression in freshly isolated cerebrovasculature from 1) r-mTBI mice (12 months post-last injury), 2) PDGFR β (+/-) mice and wild-type littermates, and 3) PSAPP mice and wild-type littermates. Lysates were analyzed for caveolin-1 by ELISA and normalized to total protein using the BCA assay. Values represent mean \pm SEM and are expressed as a percentage of each respective r-sham or wild-type littermate. The sample sizes for the r-sham and r-mTBI groups were the same for the 12 month timepoint (n = 4 each). PDGFR β (+/-) and wild-type littermates (n = 4 each) and PSAPP and wild-type littermates (n = 6 each). *P < 0.05 compared to each respective r-sham or wild-type littermate as determined by two-way ANOVA and Bonferroni's multiple comparisons test.

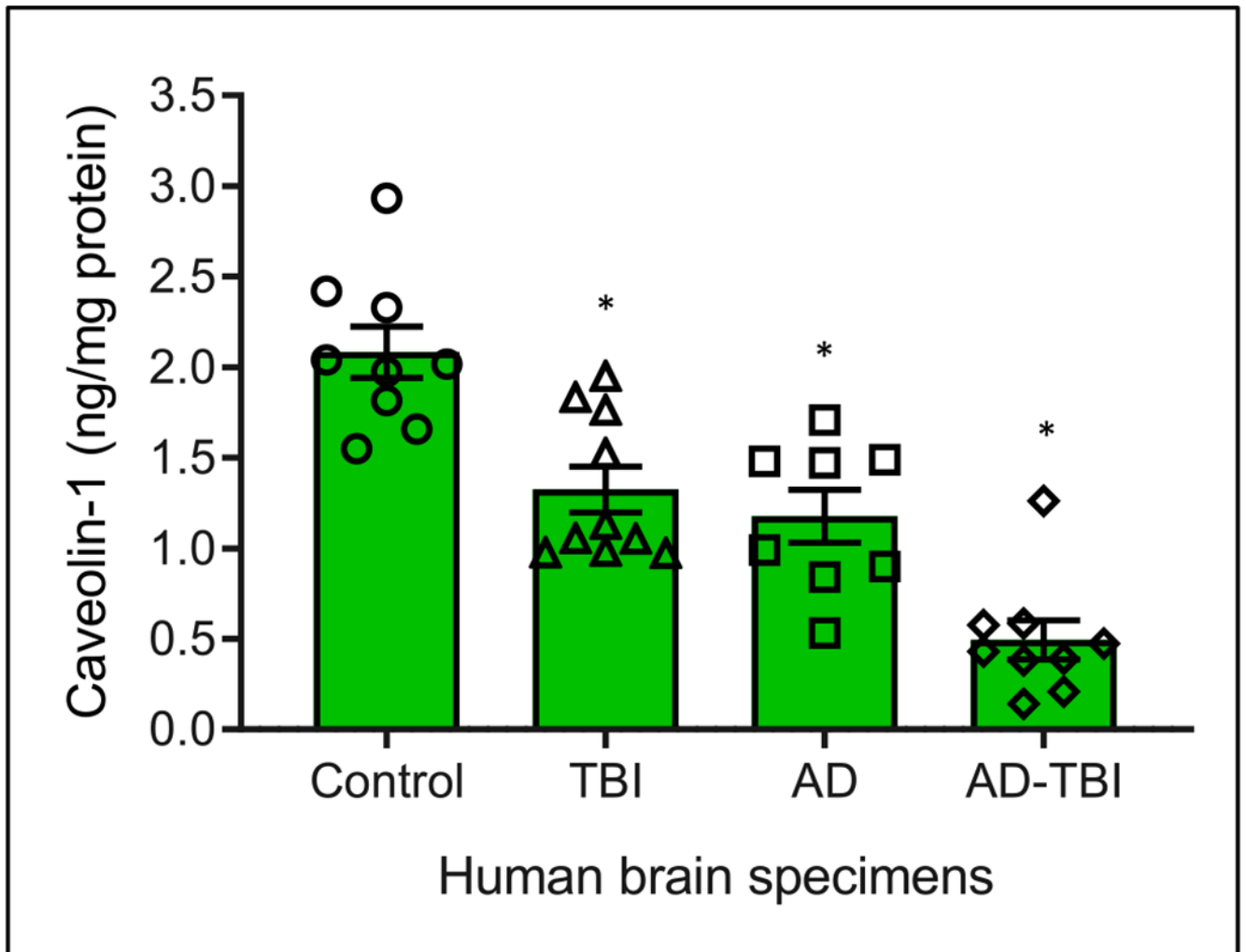


Fig. 11. Caveolin-1 expression in cerebrovasculature isolated from human brain cortex derived from, 1) non-demented control subjects (no history of TBI or AD diagnosis), 2) TBI, 3) AD, and 4) TBI and AD. Lysates were analyzed for caveolin-1 by ELISA and normalized to total protein using the BCA assay. Values represent mean \pm SEM and are expressed as ng per mg of total protein. Control ($n = 9$), TBI ($n = 10$), AD ($n = 8$), TBI-AD ($n = 9$). * $P < 0.05$ compared to control as determined by the Kruskal-Wallis test followed by Dunn's multiple comparisons test.

Table 1

Characteristics of human brain specimens.

| Group | Sample size | Age \pm SEM (years) | Sex (M/F) | Years post-last injury \pm SEM |
|--------------|--------------------|---|------------------|--|
| Control | 15 | 79.4 \pm 1.9 | 8/7 | |
| TBI | 12 | 85.2 \pm 1.9 | 6/6 | 38.1 \pm 9.2 |
| AD | 15 | 82.5 \pm 1.7 | 7/8 | |
| AD-TBI | 14 | 79.6 \pm 2.3 | 7/7 | 41.5 \pm 7.9 |